



Evolutions of antibiotic resistance genes (ARGs), class 1 integron-integrase (*int1*) and potential hosts of ARGs during sludge anaerobic digestion with the iron nanoparticles addition

Yanru Zhang^{a,b}, Zhaohui Yang^{a,b,*}, Yiping Xiang^{a,b}, Rui Xu^{a,b,c}, Yue Zheng^d, Yue Lu^{a,b}, Meiyong Jia^{a,b}, Saiwu Sun^{a,b}, Jiao Cao^{a,b}, Weiping Xiong^{a,b}

^a College of Environmental Science and Engineering, Hunan University, Changsha 410082, PR China

^b Key Laboratory of Environmental Biology and Pollution Control, Hunan University, Ministry of Education, Changsha 410082, PR China

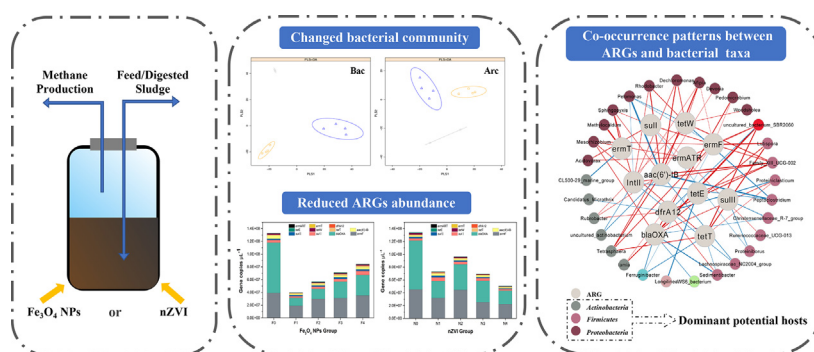
^c Guangdong Key Laboratory of Integrated Agro-environmental Pollution Control and Management, Guangdong Institute of Eco-environmental Science Technology, Guangzhou 510650, PR China

^d CAS Key Laboratory of Urban Pollutant Conversion, Institute of Urban Environment, Chinese Academy of Sciences, Xiamen 361021, China

HIGHLIGHTS

- Iron NPs promoted methane production and organic matter degradation in anaerobic digestion.
- Iron NPs changed microbial communities and reduced microbial diversity in anaerobic digestion.
- The absolute abundance of total ARGs decreased in the anaerobic digestion with iron NPs.
- *Proteobacteria*, *Firmicutes* and *Actinobacteria* were potential hosts of ARGs.
- The potential host of ARGs was the main driving factor for the fate of ARGs and *int1*.

GRAPHICAL ABSTRACT



ARTICLE INFO

Article history:

Received 12 January 2020

Received in revised form 25 March 2020

Accepted 25 March 2020

Available online 26 March 2020

Editor: Yifeng Zhang

Keywords:

Antibiotic resistance genes
Mesophilic anaerobic digestion
Network co-occurrence
Iron nanoparticles

ABSTRACT

In this work, we investigated the impact of iron nanoparticle, including magnetite nanoparticles (Fe₃O₄ NPs) and nanoscale zero-valent iron (nZVI), on the anaerobic digestion (AD) performance. Moreover, the evolutions of antibiotic resistance genes (ARGs), class 1 integrons-integrase (*int1*) and potential hosts of ARGs were also investigated. The optimal addition of Fe₃O₄ NPs and nZVI to promote methane production was 0.5 g/L and 1 g/L, which led to 22.07% and 23.02% increase in methane yield, respectively. The degradation rate of organic matter was also enhanced with the addition of Fe₃O₄ NPs or nZVI. The results of high-throughput sequencing showed that the reactors with iron NPs exhibited significant differences in microbial community structure, compared to the reactors with the non-iron NPs. Iron NPs have caused the relative abundance of the dominant bacteria (*Proteobacteria*, *Firmicutes* and *Actinobacteria*) generally decreased, while the dominant archaea (*Euryarchaeota*) increased in AD sludge. Quantitative PCR results revealed that iron NPs accelerated the reductions in total absolute abundance of ARGs, especially a beta-lactamase resistance encoded gene (*blaOXA*). Network analysis displayed that the

* Corresponding author at: College of Environmental Science and Engineering, Hunan University, Changsha 410082, PR China.
E-mail address: yzh@hnu.edu.cn (Z. Yang).

Potential hosts

attenuation of ARGs was mainly attributed to the decline of potential hosts (Proteobacteria, Firmicutes and Actinobacteria). Meanwhile, environmental factors (such as pH, soluble chemical oxygen demand and heavy metals) were also strongly correlated with ARGs.

© 2018 Published by Elsevier B.V.

1. Introduction

The contamination caused by the antibiotics and the related antibiotic resistance genes (ARGs) has been the research focus on environmental pollution and human health risks (Organization, 2015). ARGs have been transferred from environment to human commensals and pathogens due to the abuse of antibiotics and selection with antimicrobial agents, reducing the therapeutic potential of antibiotics for human and animal pathogens (Wright, 2010). Wastewater treatment plants (WWTPs) were considered as the reservoir of ARGs. WWTPs could reduce the load of antibiotics and pathogens of the receiving environments while the overall risk was not decreased (Ahmed et al., 2018; Jia et al., 2020). The ARGs in WWTPs effluent and waste activated sludge may increase due to selection pressure of antibiotics and the preferential survival of antibiotic resistance bacteria (ARBs) (Munck et al., 2015). The vertical gene transfer caused by the reproduction of bacterial host and the horizontal gene transfer caused by the mobile gene elements (MGEs) were two main modes of ARGs proliferation (Miller et al., 2015). The waste activated sludge of WWTPs has many features, such as large microbial density, high nutrient content and subinhibitory concentrations of antibiotics. Therefore the waste activated sludge could provide comfortable environment for the selection of antibiotic resistant bacteria or the horizontal gene transfer of ARGs (Qiao et al., 2017). It is essential to evaluate the fate of ARGs and MGEs in existing waste activated sludge treatment processes of WWTPs. Furthermore, finding effective ways to attenuate ARGs in waste activated sludge is also essential to limit ARGs spread to the environment.

Anaerobic digestion (AD) has been chosen as a common treatment method of waste activated sludge due to its advantage in renewable bioenergy production and pollutant removal (Rasheed et al., 2016). It could biologically convert chemical energy into methane-rich biogas, which was a substitute fuel for industry (eng, 2015). AD could also slow down the spread of antibiotics and ARGs in waste activated sludge (Diehl and Lapara, 2010b). In the process of sludge AD, the operation conditions (e.g., pH, temperature and hydraulic retention time) caused different influences in fate of ARGs (Tong et al., 2018). The change of bacterial community in different AD operation conditions might cause the distinct fate of ARGs, especially the ARGs hosts (Xiang et al., 2019; Xu et al., 2018a). However, it has been found that traditional AD might exhibit poor performance in ARGs removal. In mesophilic AD, ARGs cannot be effectively removed if the pathogens and gene transfer elements were not effectively inhibited (Sui et al., 2016). The AD residue still plays an important role in to the proliferation and propagation of ARGs (Huang et al., 2019). Before the digested sludge was utilized, controlling ARGs diffusion in waste activated sludge was crucial (Diehl and Lapara, 2010a). Moreover, due to the poor biodegradability of waste activated sludge and the low biogas production, a cost-effective approach must be developed for simultaneously enhancing methane production and removing ARGs from the AD sludge.

Iron nanoparticles (NPs) can promote the hydrolysis-acidification process of AD, improve the biogas production and realize the harmless treatment of waste activated sludge (Zhang et al., 2019b). Therefore, iron NPs were widely used in AD as the cheap pollutant absorber and a strong reductant (Xu et al., 2019; Zhang et al., 2019b). It has been proved that magnetite nanoparticles (Fe_3O_4 NPs) could promote the formation of syntrophic methane by accelerating the direct interspecies electron transfer (Holmes et al., 2017). Nanoscale zero-valent iron (nZVI) could also promote methane production by releasing hydrogen during the nZVI corrosion/oxidation process. The released hydrogen

was considered as the electronic donor of methanogenic bacteria (Jing et al., 2018). In addition, research has shown that addition of iron NPs could raise the microbial activity, alter the distribution of dominant bacteria, and ultimately improve the methane production efficiency during the AD process (Zhang et al., 2017). It has been proved that some bacteria were the carriers of ARGs. For example, *Enterococcus* might be the potential host of the ARGs and could encode erythromycin ribosome methylase (Li et al., 2015). As the potential host of ARGs, the succession of microbial community is the main factor for the variation of ARGs abundance. Based on the network analyses, researchers have found that five bacterial genera, including *Corynebacterium_1*, *Acinetobacter*, *Solibacillus*, *Enterococcus*, and *Facklamia*, were the most common hosts for selected ARGs (such as *ermB*, *sul1*, and *dfrA7*) (Song et al., 2017). And the decline in the abundances of *ermB*, *sul1*, and *dfrA7* might be related to the decrease of *Corynebacterium_1*. ARGs-carrying microbial communities may react variously with the addition of Fe_3O_4 NPs or nZVI in AD, which may lead to variations in ARGs abundance. Studies have confirmed that both Fe_3O_4 NPs and nZVI caused the ARGs attenuation in the AD of swine manure. Particularly, the addition of iron NPs is a potential mean of tetracycline resistance gene attenuation (Zhang et al., 2019a).

Adding Fe_3O_4 NPs and nZVI into AD system of waste activated sludge was an effective technique for organic matter degradation and antibiotics removal (Xu et al., 2019; Zhang et al., 2019b). Nevertheless, the evolution of microbial community, the determination of the ARGs abundance and the fate of bacteria carrying-ARGs in AD sludge caused by the addition of iron NPs have not been well understood. Thus, it is necessary to systematically study the process of AD sludge added with Fe_3O_4 NPs or nZVI to assess the performance of AD, explore the fate of microbial community, ARGs and MGEs and identify the potential hosts of ARGs. The correlation between physicochemical properties and ARGs abundance of AD sludge should also be considered. The purpose of this study was to (i) understand the influence of Fe_3O_4 NPs or nZVI on AD performance; (ii) explore the fate of microbial community ARGs, and *int1*; (iii) identify the potential host of ARGs and explain the mechanism of ARGs abundance variation; and (iv) investigate the relationship between ARGs and parameters of AD sludge. Eleven frequently detected genes were selected for quantitative analysis, including *tetW*, *tetT*, *tetE*, *ermF*, *ermT*, *ermATR*, *sull*, *sullI*, *blaOXA*, *dfrA12* and *aac(6')*-IB. *int1* was also quantified to study the potential of horizontal gene transfer. This work could bring novel insights for exploring the fate of ARGs in AD system with iron NPs.

2. Materials and methods

2.1. Pretreatment of sludge and iron NPs

The feed sludge used in this work was a mixture of secondary sludge and dewatered sludge, which was collected from a municipal WWTP in Changsha, China. After collecting the sludge, part of secondary sludge was domesticated to be seed sludge at 35 °C to obtain the mesophilic methanogenic bacteria. Both the feed and seed sludge were filtrated by the stainless-steel net (2.0 mm). Total solids (TS) and volatile solids (VS) concentration of the feed sludge were $8.19 \pm 0.09\%$ and $4.77 \pm 0.06\%$, respectively, with the pH of 7.17 ± 0.01 . TS and VS concentration of the seed sludge were $1.58 \pm 0.06\%$ and $0.79 \pm 0.01\%$, respectively, with the pH of 6.79 ± 0.02 (Table 1). The other characteristics of seed and feed sludge were also summarized in Table 1. The iron nanoparticles were nZVI (diameter of 50 nm, purity 99.9%) and Fe_3O_4 NPs

Table 1
Main characteristics of feed sludge and seed sludge used in this study.

Parameter	Feed	Seed
Volume (mL d ⁻¹)	150.00	-
pH	7.17 ± 0.005	6.79 ± 0.015
Moisture (%)	91.84 ± 0.089	98.45 ± 0.056
TS (%)	8.193 ± 0.089	1.577 ± 0.056
VS (%)	4.772 ± 0.059	0.788 ± 0.000
SCOD (g/L)	9.47 ± 0.033	0.44 ± 0.042
C/N (w/w)	62.33 ± 7.8	80.00 ± 5.3
NH ₄ ⁺ -N (g/L)	65,804.93 ± 4341.98	29,101.08 ± 792.98
<i>sull</i> ^a	(2.28 ± 0.10) × 10 ⁻¹	-
<i>sullI</i> ^a	(2.56 ± 0.22) × 10 ⁻²	-
<i>acc(6')</i> -Ib ^a	(8.05 ± 0.79) × 10 ⁻²	-
<i>dfrA12</i> ^a	(9.28 ± 0.48) × 10 ⁻⁴	-
<i>blaOXA</i> ^a	(3.97 ± 0.40) × 10 ⁻¹	-
<i>tetT</i> ^a	(3.22 ± 0.33) × 10 ⁻³	-
<i>tetE</i> ^a	(5.55 ± 0.20) × 10 ⁻³	-
<i>tetW</i> ^a	(1.96 ± 0.68) × 10 ⁻³	-
<i>ermF</i> ^a	(3.60 ± 0.23) × 10 ⁻⁵	-
<i>ermT</i> ^a	(1.04 ± 0.11) × 10 ⁻⁵	-
<i>ermATR</i> ^a	(2.60 ± 0.42) × 10 ⁻²	-
<i>intI1</i> ^a	(3.11 ± 0.31) × 10 ⁻²	-

^a The relative abundance of ARGs was normalized by total 16S rRNA gene numbers.

(diameter of 20 nm, purity >99.5%). Fe₃O₄ NPs and nZVI were purchased from Macklin Biochemical Technology Co., Ltd., Shanghai.

2.2. Continuous stirred-tank reactors (CSTRs) construction and operation

The CSTRs were divided into the nZVI group and the Fe₃O₄ NPs group. Five test dosages of Fe₃O₄ NPs (0, 0.5, 1, 2, 4 g/L) were assessed in the exposure experiments, namely F0, F1, F2, F3, F4. Similarly, five test dosages of nZVI (0, 0.5, 1, 2, 4 g/L) were added into separate reactor labeled as N0, N1, N2, N3, N4. The digesters were 5 L serum bottles with 3 L working volume. The working volume included 2 L of seed sludge and 1 L feed sludge initially. The butyl stoppers were used to capped digesters. All digesters were pre-operated for 20 days at mesophilic (37 ± 1 °C) by circulating hot water around the flask. After the biogas production was stabilized, different doses of iron NPs were added to the digesters of the experimental group every day, and these digesters were operated for 100 days. In these digesters, 150 mL of digested sludge was removed and then the feed sludge of equal volume was refilled every day to maintain a hydraulic retention time of 20 days and a constant working volume. The feed sludge and iron NPs were added to the AD reactor with a 150 mL syringe. The AD reactors were placed in a shaker to mix the digesters and iron NPs.

2.3. Sample collection and chemical analysis

The samples of digested sludge were collected on day 0, 20, 40, 60, 80, 100, respectively. The samples collected on day 100 were divided into two portions. One portion of each sample was freeze-dried in a vacuum freeze dryer for DNA extraction, and the other portion was used for chemical analysis, including pH, TS, VS, NH₄⁺-N, volatile fatty acids (VFAs), soluble chemical oxygen demand (sCOD), total organic carbon (TOC), total polysaccharides and heavy metal. Sludge samples collected on day 0, 20, 40, 60, 80, 100 were measured to monitor the dynamic changes of ARGs and *intI1*.

The biogas production and pH value of all anaerobic reactors were measured daily. The pH was measured using a pH meter (Mettler Toledo). Daily biogas production was measured by the drainage method. The determination of biogas compositions was determined by a gas chromatography (GC-2014, Shimadzu, Kyoto, Japan). The gas chromatography is composed of a 2 m × 4 mm stainless steel column (GDX-101, Bio-Rad, Berkeley, CA, USA) and a thermal conductivity detector.

TOC, sCOD, TS, VS, total polysaccharide, NH₄⁺-N and C/N were determined through Standard Methods (Eaton, 2005). The content of VFAs was determined by a gas chromatograph (Agilent 7890A, USA) with a flame ionization detector (FID) and a DB-1 DB-FFAP (Agilent, USA) column (30 m × 0.32 mm × 0.50 μm). In addition, the sludge samples were freeze-dried and grounded to sieve through 100 mesh. Each treated sludge sample (0.2 g) was added into a 10 mL mixture of aqua regia and hydrofluoric acid (3:1,v/v) according to the microwave assisted digestion method 3051A (EPA, 2007), and a microwave digestion apparatus (Mars 5, CEM, USA) was used for digestion. The concentrations of heavy metals including Cu, Zn, Cr, Pb, Cd, and Ni were determined by inductively coupled plasma mass spectrometry (ICP-MS). Each sample was tested in triplicate.

2.4. DNA extraction and high-throughput sequencing

The total genomic DNA of each dried sludge sample (0.2 g) was extracted by the E.Z.N.A.® Soil DNA Kit (Omega Bio-tek, Norcross, GA, USA) according to the manufacturers' protocols. DNA samples were amplified by PCR and the amplified products were purified by an AxyPrep DNA Gel Extraction Kit (Axygen Biosciences, Union City, CA, USA). The purified amplicons obtained above were polymerized in equimolar concentrations and paired-end sequenced (2 × 250) on an Illumina MiSeq PE250 platform with MiSeq Reagent Kit v3 at Shanghai Personal Biotechnology Co., Ltd., Shanghai, China (Xu et al., 2019; Xu et al., 2018b). The bacterial community was analyzed by the primers 524F (5'-ACTCCTACGGGAGGCAGCA-3')/958R (5'-GGACTACHVGGGTWTCTAAT-3') targeting the V3-V4 hyper variable regions. And the primers 338F (5'-TGYCAGCCGCGGTAA -3')/806R (5'- YCCGCGTGTGAVTCCAAT-3') targeting the V4-V5 hyper variable regions were selected for archaeal community analysis as described in the previous study (Yang et al., 2016b). QIIME was used to deal with the amplicon data analysis, such as quality filtering, chimerism inspection, and taxonomic classification to obtain clean sequences (Caporaso et al., 2010a). The high-quality sequences were available in the NCBI Sequence read archive under the accession number SRP199815.

2.5. Quantitative PCR (qPCR) of ARGs and *intI1*

Quantitative PCR (qPCR) is a feasible method to detect gene fragment concentrations in complex environmental samples. Therefore, qPCR was used to quantify the screened ARGs and *intI1* in this study. Three tetracycline resistances encoded genes (*tetW*, *tetT*, *tetE*), three MLSB resistance encoded genes (*ermF*, *ermT*, *ermATR*), two sulfonamides resistance encoded genes (*sull* and *sullI*), one beta-lactamase resistance encoded gene (*blaOXA*), one gene encoding other/efflux (*dfrA12*), one aminoglycoside resistance encoded gene (*aac(6')*-IB) and microbial 16S rRNA genes for archaea/bacteria were selected. *intI1*, which is a representative mobile genetic element, was also assessed to reveal the potential of horizontal gene transfer. The forward and reverse primer sequences, expected amplicon size, primer annealing temperature and resistance mechanism of gene targets selected in this study were listed in Table 1 of supplementary material (Table S1).

The qPCR of 11 selected ARGs and MGE (*intI1*) was performed on iQ5 real-time PCR thermocycler (BIO-RAD, USA) with Super Real fluorescence premixing (SYBR Green) kit. Each target gene was quantified in triplicate for each sample by the purified DNA template calibration curve, which had been amplified by conventional PCR and negative control. The reaction mixture (20 μL) was formed with 10 μL of 2 × Power PreMix (Tiangen, China), 0.6 μL of forward/reverse primer (10 μM), 1.0 μL of template DNA, and 7.8 μL of RNase-Free ddH₂O. The temperature of melting curve analysis was between 50 °C and 95 °C with 0.5 °C/30s per cycle. 16S rRNA genes for bacteria were selected as the internal reference genes to minimize the bias caused by different bacterial abundance (Xu et al., 2018a).

2.6. Statistical analysis

The clean sequences were clustered into operational taxonomic units (OTUs) at 97% sequence identity by UCLUST. The chimeric sequences were identified and removed by UCHIME (Caporaso et al., 2010b). The OTU table in QIIME was used to calculate the alpha diversity index of microorganisms, including Chao1 abundance estimation, Shannon diversity index, Simpson index and abundance-based coverage estimator (ACE). SPSS 23 (IBM, USA) software was used for analysis of variance (ANOVA) to determine the significant difference of the results among the samples, which was statistically significant when $P < 0.05$. In addition, correlation analysis was also performed by SPSS 23 (IBM, USA) to determine the relationships between the measured parameters. The bacterial genera with a correlation index higher than 0.8 ($P < 0.05$) was considered as a potential host for selected ARGs and *intl1* (Junker and Schreiber, 2008). Visualization of network analysis was produced on the Cytoscape (version 3.2.0) interactive platform. Origin 2015 and Heml 1.0 were used to conducted figures. The absolute abundance of ARGs and *intl1* were used for the co-occurrence network analysis and the correlation analysis.

3. Results and discussion

3.1. Performance of CSTRs

Generally, during the entire experiment, Fe_3O_4 NPs and nZVI could not result in the drastic alteration of pH values (ranged from 7.30 to 8.03) among these digesters (Fig. S1). Detail performances of CSTRs on day 100 were summarized in Fig. 1. Fig. 1(a) and (b) showed the influence of iron NPs on accumulative methane yield in AD process. The dose of Fe_3O_4 NPs and nZVI for the maximum accumulative methane production was 0.5 g/L (F1) and 1 g/L (N2), respectively. And the highest accumulative methane production was 112.76 L from F1 and 112.01 L from N2, which increased by 22.07% and 23.03% compared with the non-iron NPs added digesters (F0 and N0), respectively. Besides, the removal efficiency for TS and sCOD of the digesters with iron NPs was higher than the control digester. As shown in Fig. 1(c) and (d), the TS removal efficiency in F0 and N0 were 49.19% and 49.11% after anaerobic digestion for 100 days, while F1 and F2 could reach to 87.90% and 82.90%, respectively. In Fig. 1(e) and (f), a similar result occurred in non-iron NPs digesters. Removal efficiency of sCOD was only 52.99% and 52.63%, respectively. In digesters with iron NPs, the highest removal efficiency of sCOD was 85.29% (F1) and 76.20% (N2). These results showed that AD performance decreased with the increase of Fe_3O_4 NPs concentration, and 0.5 g/L Fe_3O_4 NPs was the optimum dosage in this dose-response experiment. Similarly, excessive amount of nZVI would also lead to AD performance degradation, and 1 g/L nZVI was the optimum dosage.

Iron NPs was the ideal multifunctional cofactors for many proteins because of its ability to up-take or lose electrons. The mechanism of electron transferred from nZVI to the microbe is microbial corrosion and surface oxidation through nZVI. Under anaerobic conditions, nZVI is oxidized to ferrous iron (Fe^{2+}), and further formed cathodic hydrogen ($\text{H}_2/[\text{H}]$) to synthesize the key enzymes (Srilakshmi et al., 2010). Many studies have confirmed that nZVI could effectively promote the hydrolysis and acidification process of AD sludge and stimulate the production of sCOD (Xu et al., 2019; Zhang et al., 2019b). nZVI could also maintain a reducing environment by reducing the oxidation-reduction potential and improve the conversion of complex organic compounds into VFAs. This process provided a bountiful substrate for the subsequent methane production (Su-li et al., 2011). Fe_3O_4 NPs could also release iron ions for methanogens in the anaerobic reaction process, thus increasing the activity of characteristic enzymes in the system. As a carrier of inter-specific electron transfer, Fe_3O_4 NPs could promote the metabolic process of anaerobic microorganisms, strength the utilization of

sCOD and accelerate the degradation process of organic compounds in the AD system (Pan et al., 2019). However, excessive active iron ions would have a fatal effect on methanogenic bacteria and eventually lead to the inhibition of methanogenesis (Suanon et al., 2016).

3.2. Characterization of microbial communities

In all sludge samples, Miseq sequencing of 16S rRNA amplicons yielded 481,853 effective sequences for the bacterial community, OTUs were identified into 40 phyla and 719 genera. As for the composition of the archaea community, 412,838 effective sequences were yielded, and a total of 34 genera belonged to 5 phyla were identified. Based on the diversity indices (Table 2), the bacterial diversity indices (including Shannon, Simpson, ACE and Chao-1) of samples with iron NPs addition were significantly lower than that samples without iron NPs addition. On the contrary, the iron NPs could increase the richness and diversity of the archaeal community in the AD sludge. The archaea diversity of F group was higher than the N group. No significant change ($P > .05$) in the alpha diversity of the microbial community was observed with the further increase of Fe_3O_4 NPs/nZVI doses.

After 100 days in AD, the dominant phyla of bacteria were Proteobacteria (accounting for 26.69% of total reads), Firmicutes (24.80%), and Actinobacteria (10.92%) in all CSTRs (Fig. 2(a)). Euryarchaeota was dominant among the five identified archaeal phyla and its stable range was >95% (Fig. 2(b)). As for the genus level (Table S2), the relative abundance of the top 10 genera together only accounted for 0.2%–14.4% in total bacteria composition, and most of the genera comprising <1%. *Methanosarcina* was dominant in the archaea genus (accounting for 70.60%–90.00%). Generally, the relative abundance of the top 10 bacterial genera in the digesters with Fe_3O_4 NPs/nZVI were significantly lower than that in the digesters without iron NPs (F0/N0). The abundance of *Methanosarcina* was increased in the digesters with Fe_3O_4 NPs/nZVI, which was consistent with the results of alpha diversity indices. These results also proved that biogas production in iron NPs added digesters were higher than that in the N group, because Euryarchaeota is the main methanogens. Besides, both *Methanobacterium* and *Methanosarcina* were positively correlated with biogas yield, which meant that they might be involved in the methane production process of the AD system (Wang et al., 2018).

Partial least squares discriminant analysis (PLS-DA) was used to analyze the similarity of bacterial and archaeal community composition in different samples. The results of PLS-DA showed that both the bacterial and archaeal community structure changed throughout AD sludge with the addition of Fe_3O_4 NPs/nZVI. Samples from the same treatment were more likely to cluster together. In Fig. 3(c) and (d), the digesters without iron NPs (F0 and N0), Fe_3O_4 NPs added digesters (F1, F2, F3 and F4) and nZVI added digesters (N1, N2, N3 and N4) formed distinct clusters, respectively. Thus, the addition of Fe_3O_4 NPs/nZVI in the AD system could influence microbial compositions. However, the microbial community structure did not change significantly with the increased dosage of Fe_3O_4 NPs/nZVI in mesophilic CSTRs.

These results indicated that the effect of Fe_3O_4 NPs/nZVI on the bacterial diversity of AD sludge was negative, which might be attributed to the biological toxicity on microorganisms. Fe_3O_4 NPs and nZVI could both interact with key components (such as functional proteins) of the cell membrane, which could damage cell membrane and disrupt the bacterial integrity (Yang et al., 2016a). High concentration iron ions could inhibit the formation of methane. It was probably because phosphorus is one of the key nutrients of methanogens, and the high concentration iron ions formed stable complexes with PO_4^{3-} , which led to a decrease in the amount of available phosphorus for microorganisms and the decrease of microbial abundance (Rudnick et al., 1990). Appropriate iron NPs were beneficial to from anaerobic environment which provided stable and favorable conditions for methanogenic archaea to produce methane (Liu et al., 2015).

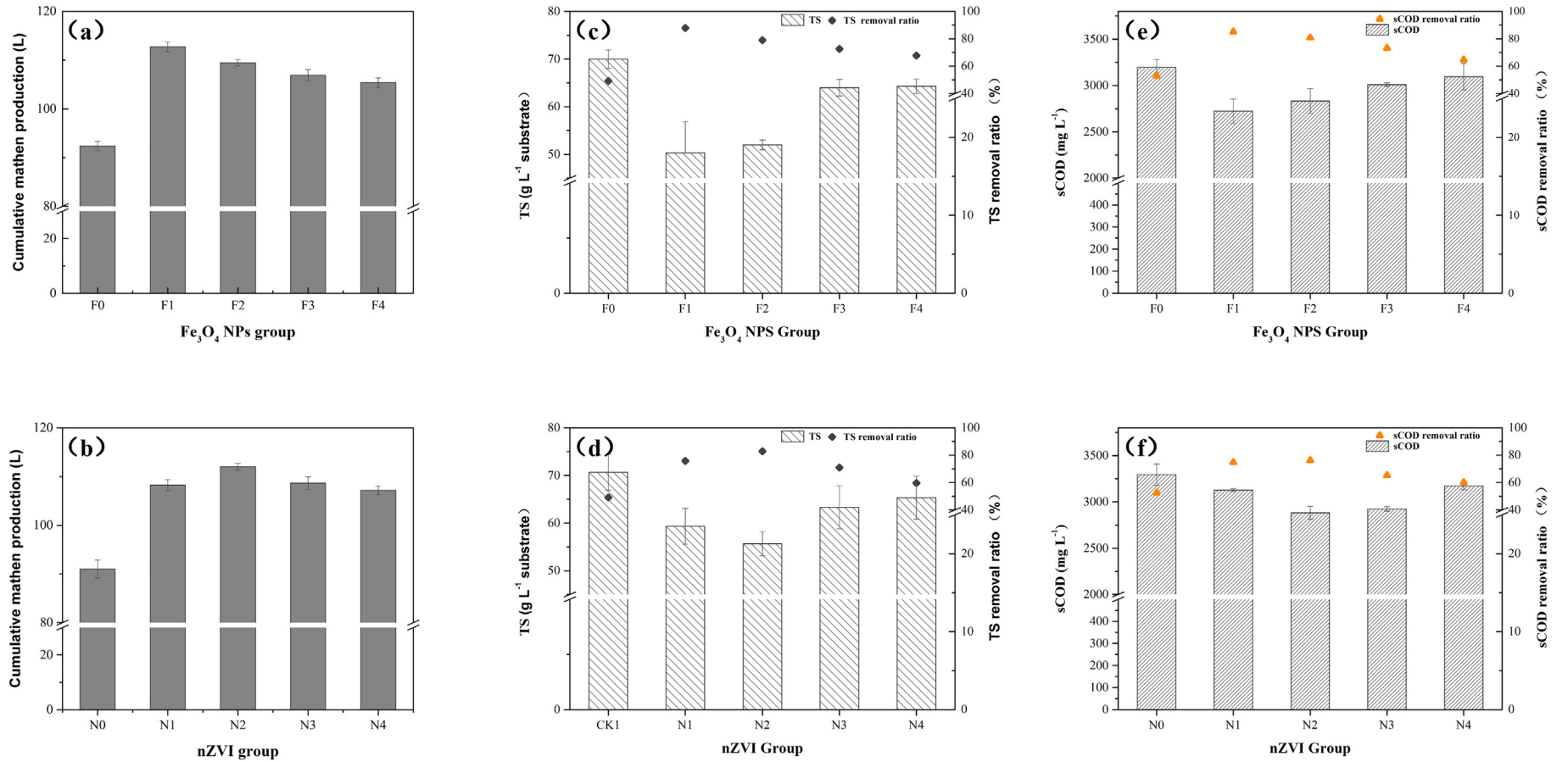


Fig. 1. General performance of CSTRs with/without iron NPs added. (a) and (b) Cumulative methane production; (c) and (d) TS content and removal rate; (e) and (f) sCOD content and removal rate.

Table 2
Microbial diversity index of CSTRs sludge.

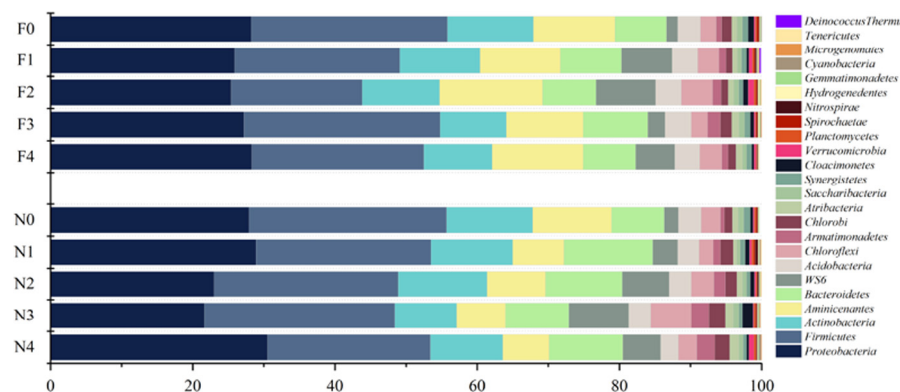
	Simpson		Chao1		ACE		Shannon	
	Bac	Arc	Bac	Arc	Bac	Arc	Bac	Arc
F0	0.99	0.36	2537.83	436.22	2569.52	449.52	8.57	1.80
F1	0.99	0.91	1654.00	673.00	1654.00	673.00	8.40	5.07
F2	0.99	0.93	1672.00	784.94	1672.00	801.70	8.44	5.51
F3	0.99	0.92	2273.88	671.00	2445.52	671.00	8.46	5.29
F4	0.99	0.91	2361.88	641.00	2446.27	641.00	8.39	5.06
N0	0.99	0.34	2548.84	431.14	2549.57	442.62	8.58	1.88
N1	0.99	0.89	2396.14	637.00	2603.05	637.00	8.47	4.84
N2	0.99	0.80	2488.05	585.00	2554.41	585.00	8.29	4.16
N3	0.99	0.83	1832.65	619.28	1927.27	623.67	8.10	4.32
N4	0.98	0.83	1600.43	606.00	1693.73	606.72	7.85	4.36

3.3. Changes of ARGs and *int1* during CSTRs

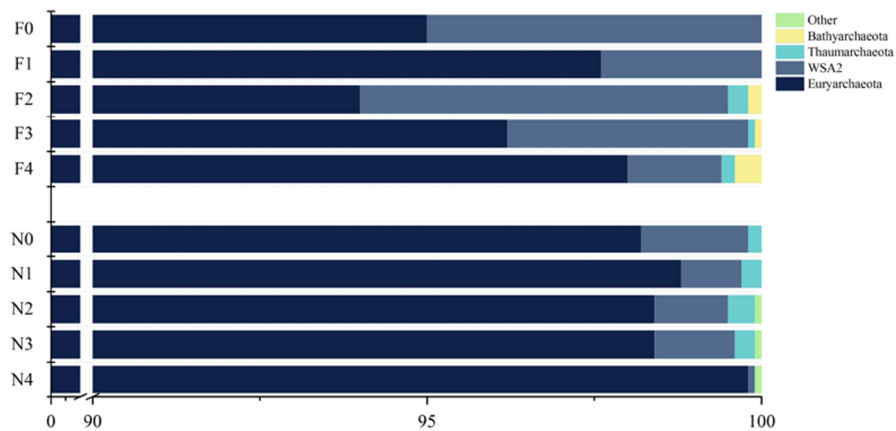
The selected ARGs abundance of the feed sludge was summarized in Table 1. Feed sludge from the WWTP is an important repository of resistance genes, which exhibited high ARGs relative abundance, especially *blaOXA*, *tetW* and *sull*. The standard curves and amplification efficiency of qPCR for selected ARGs were given in Table S3. Fig. 3 displayed the absolute abundance of total ARGs in the 100-day CSTRs. Both Fe₃O₄ NPs and nZVI could significantly reduce the absolute abundance of total ARGs. F0 (1.33 E+8 gene copies μL^{-1}) and N0

(1.34 E+8 gene copies μL^{-1}) had the highest absolute abundance of total ARGs in the F group and N group, respectively. There was a negative correlation between the total ARGs removal rate and the Fe₃O₄ NPs dosage. The ARGs removal rate of F1 was the highest, reaching 70.73%, followed by F2 (57.87%), F3 (47.67%) and F4 (37.60%). The absolute abundance of total ARGs for the N group also experienced a reduction of 28.27%–62.69% after 100 days. ARGs removal rate was the highest obvious in N4 (62.69%). Both Fe₃O₄ NPs and nZVI had the most obvious removal effect on *blaOXA* compared with other target genes, and the absolute abundance of *blaOXA* in F0 was 6.42 times of that in F1. The absolute abundance of *ermF*, *ermATR*, *sull* and *tetT* decreased in the AD reactors with the addition of iron NPs, while the absolute abundance of *sull*, *tetW* and *dfpA12* increased. The abundance of *aac(6′)-IB*, *tetE* and *ermT* did not increase or decrease significantly. These results indicated that sludge AD with iron NPs could only remove some ARGs but could not effectively remove all ARGs. Conversely, the absolute abundance of some ARGs increased after this disposal, which was corroborated with previous studies (Xu et al., 2018a).

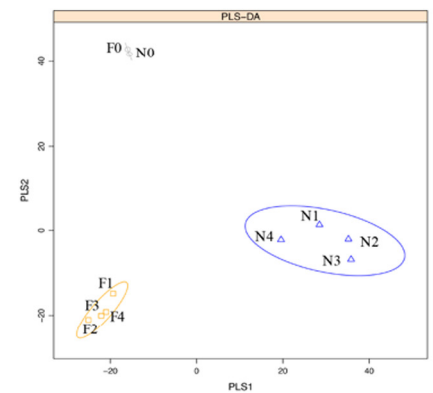
16S rRNA gene for bacteria was used to normalize the relative abundance of ARGs. Fig. 4 displayed the relative abundance changes of 11 selected ARGs and *int1* during the 100-day AD process. Variations in the prevalence of most selected ARGs displayed a similar trend over time in the AD process. In different reactors, the relative abundance of the same ARG showed an upward or downward trend with time. Iron NPs could deteriorate the enrichment of tetracycline resistance genes. Compared with the initial value (D0), gene



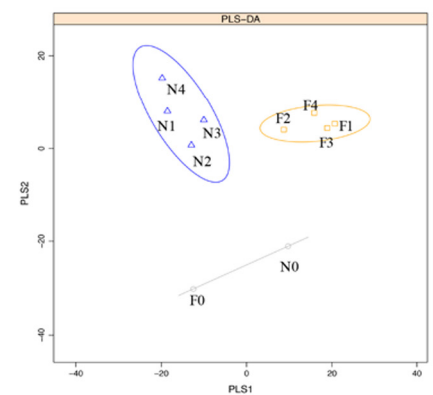
(a) The relative abundance of bacterial phylum



(b) The relative abundance of archaea phylum



(c) PLS-DA of bacterial community



(d) PLS-DA of archaea community

Fig. 2. Profiles of microbial community from CSTRs. (a) and (b) Relative abundance of microbial community at phylum level. (c) and (d) Distribution of bacterial and archaeal community composition (genus level) by PLS-DA.

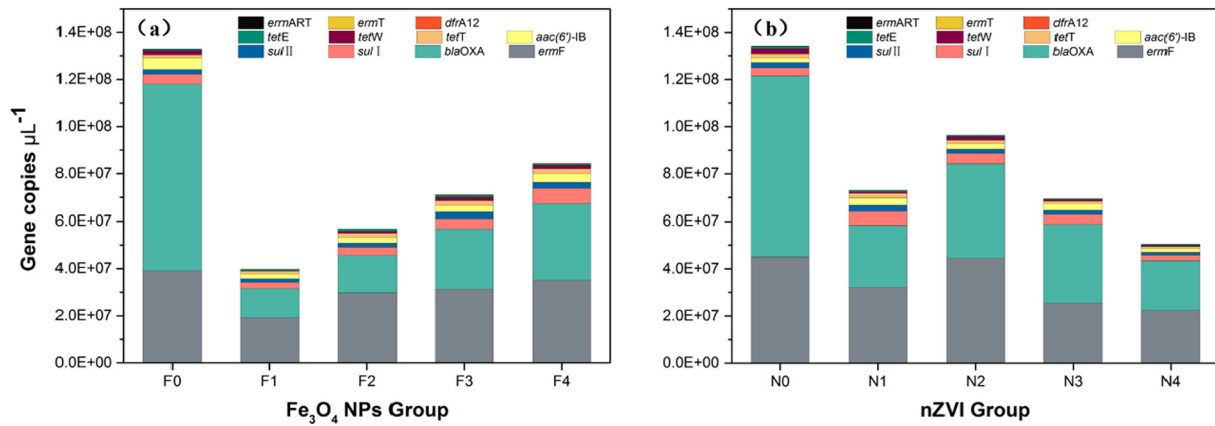


Fig. 3. The absolute gene copies of ARGs and *int1* of CSTRs with/without iron NPs added.

abundance of *tetT*, *tetE*, *tetW* reduced by 64.74%–92.37%, 80.28%–85.82%, and 91.66%–93.63% from F group. As for N group, gene abundance of *tetT*, *tetE*, *tetW* reduced by 57.96%–87.48%, 61.58%–88.58% and 93.07%–94.94%, respectively. There was a significantly removal effect of the *aac(6′)*-IB relative abundance in all the groups. The average removal rate of *aac(6′)*-IB in F group, N group and control group was 95.10%, 93.70% and 93.93%, respectively, indicating that AD had a significant effect on *aac(6′)*-IB. Although the relative abundance of *drfA12* and *int1* decreased during the AD process, the abundance of these genotypes in the iron NPs added digesters were higher than those in control digesters. Gene targets like *ermF*, *ermT*, *ermATR*, *sull*, *sullI* and *blaOXA* were found to be enriched on 100th day. It was worth noting that *sull* and *sullI* were significantly ($P < 0.05$) increased in the nZVI or the Fe_3O_4 NPs added digesters compared to the reactor without the iron NPs added. The relative abundance of *sull* and *sullI* reached the peak on the 60th day (6.25×10^{-1} for *sull* and 1.33×10^{-1} for *sullI*). Three macrolide resistance genes (*ermF*, *ermT*, *ermATR*) enriched in all CSTRs, but the abundance of three macrolide resistance genes in F0/N0 were higher than that in the digesters with iron NPs added. As for the *blaOXA*, compared with the initial value, a low concentration of Fe_3O_4 NPs (0.5 g/L and 1 g/L) could significantly reduce the relative abundance of *blaOXA*, while a high concentration of Fe_3O_4 NPs (4 g/L) and nZVI (4 g/L) could enrich *blaOXA*. Nevertheless, the abundance of *blaOXA* in digesters with iron NPs added were much lower than that in the control digesters.

Extracellular DNA can be physically destroyed by hydrolysis and biodegradation in the AD system (Mager and Thomas, 2011). Fe_3O_4 NPs had been proved to accelerate the hydrolysis acidification of AD and improve the biological reaction rate (Zhang et al., 2019a). However, the nZVI corrosion products could be deposited onto the microbial cells, and cause the deformation and damage of microbial cellular structure (Zhu et al., 2014). The addition of both nZVI and Fe_3O_4 NPs led to various variations in ARGs abundance, which presumably ascribing to ARGs coded for different resistance mechanisms. For example, the removal performance of *tet* genes encoding tetracycline resistance was similar because *tetE* encode for tetracycline efflux, *tetT* and *tetW* encode for ribosomal protection, iron NPs can disable these two resistance mechanisms (Chopra and Roberts, 2001). Some ARGs with increased abundance, which host different bacteria, may share resistance through the same mechanism, e.g., *blaOXA* and *aac(6′)*-IB with *Lutispora* and *Rhodobacter*, respectively (Diehl and Lapara, 2010b). The other reason for the variations of ARGs could be associated with bacterial community succession caused by iron NPs. In previous studies, nZVI and nanomagnetite decreased the abundance of bacteria belonging to

Firmicutes, which was the host for ARGs (Shi et al., 2019). Therefore, the bacterial community structure changed and the ARGs abundance reduced. There was a co-occurrence pattern of bacteria and ARGs, which indicated that the evolution of the bacterial community might be the key driving factor for the fate of ARGs.

3.4. Co-occurrence among ARGs, *int1*, and potential hosts

11 selected ARGs, *int1* and 152 bacterial genera were combined to explore the co-occurrence patterns between ARGs and bacterial taxa. The potential hosts of ARGs and *int1* had also been explored. The co-occurrence patterns were visualized by network analysis. As shown in Fig. 5, 30 genera (belong to 7 phyla) were identified as the potential hosts for selected ARGs and *int1*. Specifically, most identified bacteria genus (>80%), which belonged to Proteobacteria, Firmicutes and Actinobacteria, were significantly ($P < 0.05$) related to selected ARGs and *int1*. These bacteria phyla were frequently related to antibiotic resistance in existing studies (Liao et al., 2018; Wu et al., 2017). The dominant *int1*-associated genera belonging to the phyla of Firmicutes and Bacteroidetes were *Family_XIII_UCG-002* ($P = 0.043$) and *Sphingopyxis* ($P = 0.044$), respectively. These genera also exhibited high connectivity with *sull* and *aac(6′)*-IB. The *aac(6′)*-IB had the most potential hosts (8) followed by *ermF* (7), *tetW* (7), *blaOXA* (6) and *tetT* (5). Different ARGs exhibited a significant positive correlation with the same host, indicating that multiple resistance existed in AD sludge widely.

It was reported that the bacterial community composed of Firmicutes and Actinobacteria might be the reason for carrying and transmitting ARGs, and some bacteria could even synthesize antibiotics (Huerta et al., 2013). Some potential host bacteria have been annotated, for example, *Acinetobacter* was elucidated to be the host of *blaOXA* (Jia et al., 2017). As the potential hosts, Proteobacteria, Firmicutes and Actinobacteria, were reduced in abundance in the CSTRs with iron NPs added (Fig. 4). Therefore, the addition of iron NPs showed a better ARGs reduction performance, which was related to the destruction of host bacteria by iron NPs. The result was consistent with the previous study that the addition of iron NPs in AD system led to the decrease of bacterial community diversity index, so that the host bacterial range of ARGs was reduced, and eventually the removal of ARGs abundance would be promoted (Ma et al., 2011). In addition, most ARGs were not significantly correlated with *int1*, only *sull* ($P = 0.004$), *aac(6′)*-IB ($P = 0.003$) and *tetE* ($P = 0.022$) were significantly positively correlated with *int1* in this study (Table 3). The result might indicate a lower frequency of horizontal gene transfer caused by iron NPs. In conclusion, network analysis revealed that the evolution in the bacterial community was the main factor for the changed ARGs in the AD system with Fe_3O_4 NPs/nZVI.

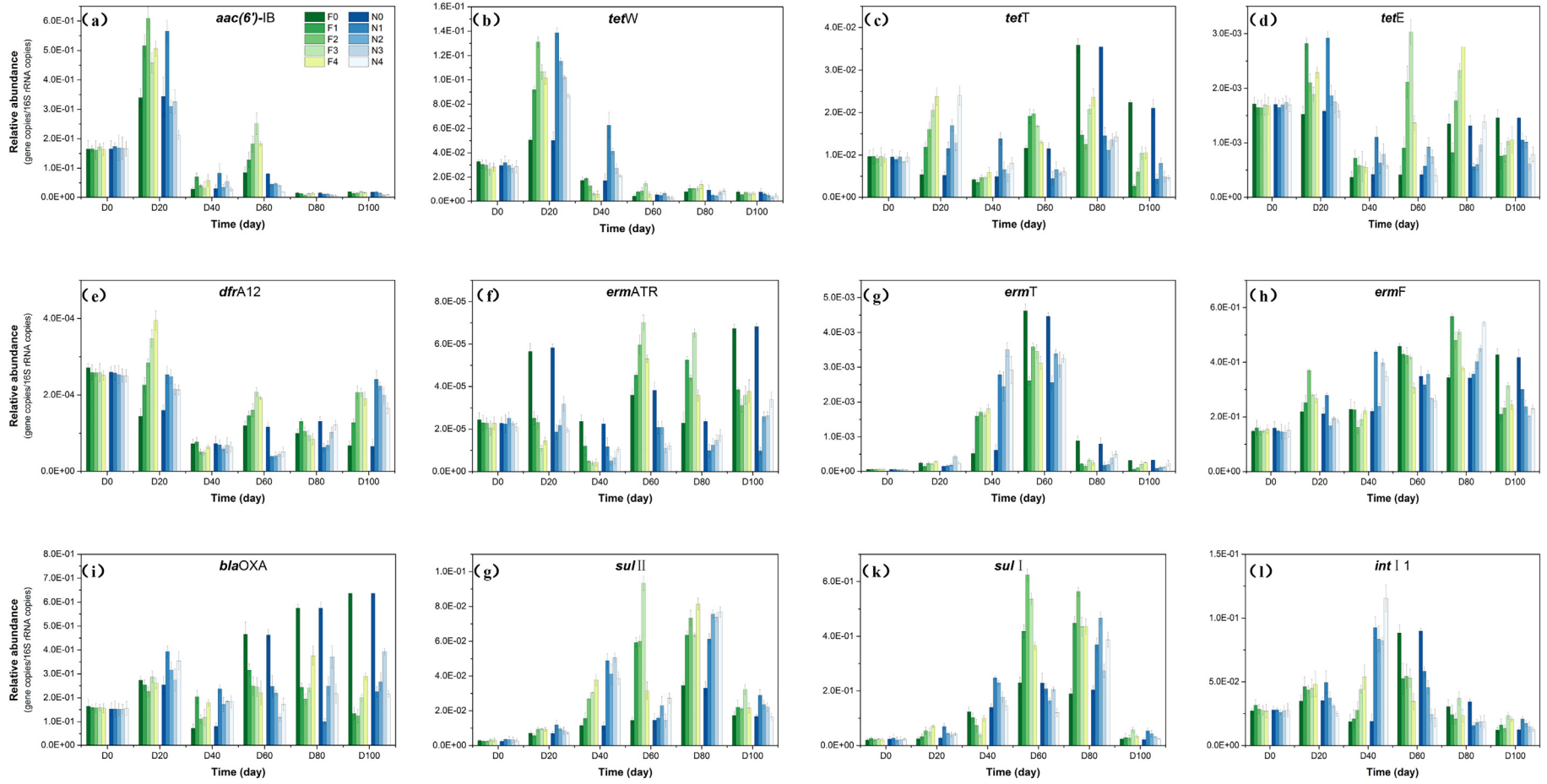


Fig. 4. Dynamic change of target genes and *int1* relative abundance during the AD process in all reactors. The quantity of ARGs detected in this study was normalized by the 16S rRNA gene copies to minimize the basis caused by different microbial abundance.

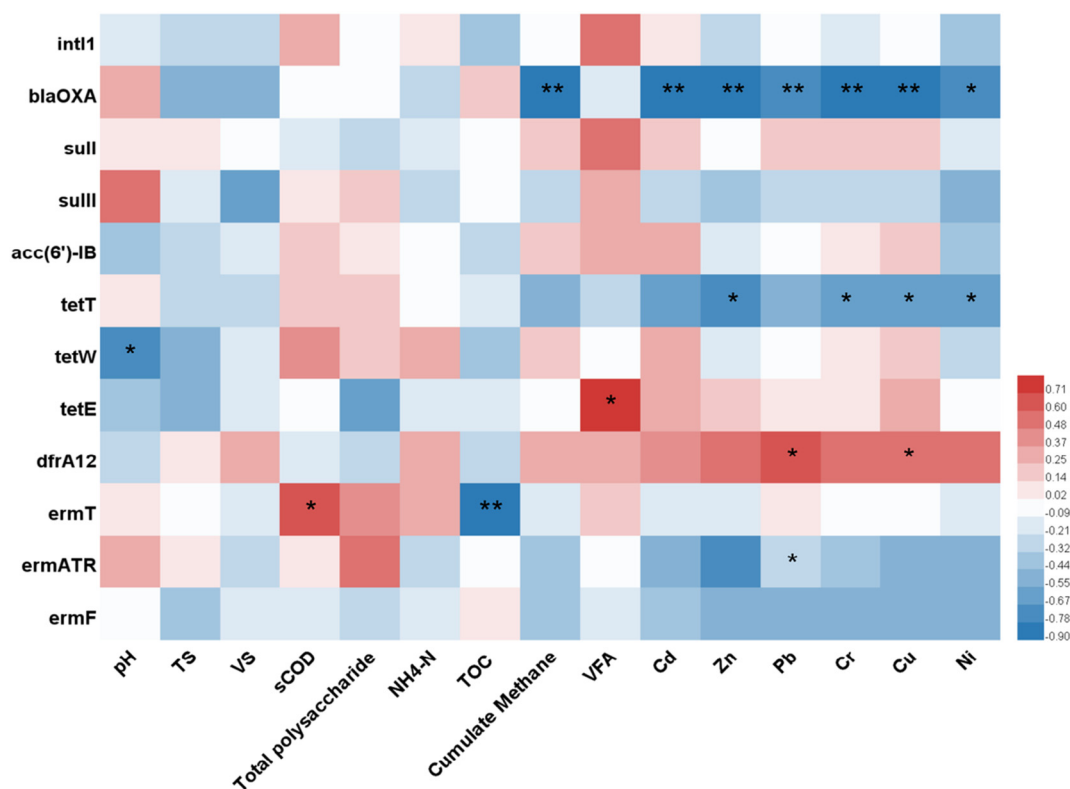


Fig. 6. Heatmap based on the relationship between ARGs, *intl1* and sludge characteristics. Color intensity shows the correlation between each factor, as shown by the color key at the bottom right.

heavy metals can also select and stimulate antibiotic resistance via both co-resistance and cross-resistance mechanisms (Zhao et al., 2019). The influence of metal toxicity on the amount of detected ARGs accounted for 78% and the influence of metal toxicity on the co-occurring ARGs abundance via MGEs accounted for 69% of the total influence in the previous study (Zhao et al., 2019). The presence and transfer of ARGs in AD sludge were partially driven by heavy metals, so there was a significant correlation between ARGs and heavy metals.

4. Conclusions

The AD performance was optimized when iron NPs was added properly. Iron NPs could stimulate the attenuation of the total absolute abundance of ARGs, especially a beta-lactamase resistance encoded gene (*blaOXA*). Iron NPs also reduced microbial diversity and changed microbial community structure in AD sludge. Network analysis showed that three dominant bacteria phyla (Proteobacteria, Firmicutes and Actinobacteria) were also the main potential hosts of ARGs. Therefore, the succession of bacterial community was the major reason to explain the attenuation of ARGs abundance. Meanwhile, bacterial populations carrying ARGs responded to different sludge physicochemical properties (e.g., pH, sCOD and heavy metals).

CRedit authorship contribution statement

Yanru Zhang: Conceptualization, Methodology, Software, Writing - original draft, Validation, Investigation, Formal analysis. **Zhaohui Yang:** Conceptualization, Supervision, Project administration, Funding acquisition. **Yinping Xiang:** Investigation, Software, Data curation. **Rui Xu:** Software, Data curation. **Yue Zheng:** Formal analysis, Writing - review & editing. **Yue Lu:** Formal analysis, Writing - review & editing. **Meiying**

Jia: Formal analysis, Writing - review & editing. **Saiwu Sun:** Writing - review & editing. **Jiao Cao:** Writing - review & editing. **Weiping Xiong:** Writing - review & editing.

Declaration of competing interest

The authors declare that they have no known competing financial interests or personal relationships that could have appeared to influence the work reported in this paper.

Acknowledgments

The study was financially supported by the National Natural Science Foundation of China (51878258, 51521006 and 51709100).

Appendix A. Supplementary data

Supplementary data to this article can be found online at <https://doi.org/10.1016/j.scitotenv.2020.138248>.

References

- Ahmed, W., Zhang, Q., Lobos, A., Senkbeil, J., Sadowsky, M.J., Harwood, V.J., et al., 2018. Precipitation influences pathogenic bacteria and antibiotic resistance gene abundance in storm drain outfalls in coastal sub-tropical waters. *Environ. Int.* 116, 308–318.
- Caporaso, J.G., Kuczynski, J., Stombaugh, J., Bittinger, K., Bushman, F.D., Costello, E.K., et al., 2010a. QIIME allows analysis of high-throughput community sequencing data. *Nat. Methods* 7, 335–336.
- Caporaso, J.G., Kuczynski, J., Stombaugh, J., Bittinger, K., Bushman, F.D., Costello, E.K., et al., 2010b. QIIME allows analysis of high-throughput community sequencing data. *Nat. Methods* 7, 335.
- Chopra, I., Roberts, M., 2001. Tetracycline antibiotics: mode of action, applications, molecular biology, and epidemiology of bacterial resistance. *Microbiology & Molecular Biology Reviews* 65, 232–260.

- Diehl, D.L., Lapara, T.M., 2010a. Effect of temperature on the fate of genes encoding tetracycline resistance and the integrase of class 1 integrons within anaerobic and aerobic digesters treating municipal wastewater solids. *Environmental Science & Technology* 44, 9128–9133.
- Diehl, D.L., Lapara, T.M., 2010b. Effect of temperature on the fate of genes encoding tetracycline resistance and the integrase of class 1 integrons within anaerobic and aerobic digesters treating municipal wastewater solids. *Environmental Science & Technology* 44, 9128–9133.
- Eaton, A., 2005. Standard Methods for the Examination of Water and Wastewater. *Environmental Protection and Resource Recovery*.
- EPA U, 2007. Microwave assisted acid digestion of sediments, sludges, soils, and oils. SW-846 method A 3051, 1997.
- Holmes, D.E., Shrestha, P.M., Walker, D.J., Dang, Y., Nevin, K.P., Woodard, T.L., et al., 2017. Metatranscriptomic Evidence for Direct Interspecies Electron Transfer Between *Geobacter* and *Methanotrix* Species in Methanogenic Rice Paddy Soils. 83(AEM) (00223–17).
- Huang, X., Zheng, J., Tian, S., Liu, C., Liu, L., Wei, L., et al., 2019. Higher temperatures do not always achieve better antibiotic resistance genes removal in anaerobic digestion of swine manure. *Appl. Environ. Microbiol.* 85.
- Huerta, Belinda, Marti, Elisabet, Gros, Meritxell, et al., 2013. Exploring the links between antibiotic occurrence, antibiotic resistance, and bacterial communities in water supply reservoirs. *Sci. Total Environ.* 456–457, 161–170.
- Jia, B., Raphenya, A.R., Alcock, B., Wagglechner, N., Guo, P., Tsang, K.K., et al., 2017. Expansion and model-centric curation of the comprehensive antibiotic resistance database. *Nucleic Acids Res.* 45, D566–D573.
- Jia, M., Yang, Z., Xu, H., Song, P., Xiong, W., Cao, J., et al., 2020. Integrating N and F doped TiO₂ nanotubes with ZIF-8 as photoelectrode for enhanced photoelectrocatalytic degradation of sulfamethazine. *Chem. Eng. J.* 388, 124388–124399.
- Jing, W., Hao, X., Loosdrecht, M.C.M.V., Ji, L., 2018. Feasibility analysis of anaerobic digestion of excess sludge enhanced by iron: a review. *Renew. Sustain. Energy Rev.* 89, 16–26.
- Junker, B.H., Schreiber, F., 2008. Analysis of Biological Networks.
- Li, B., Yang, Y., Ma, L., Ju, F., Guo, F., Tiedje, J.M., et al., 2015. Metagenomic and network analysis reveal wide distribution and co-occurrence of environmental antibiotic resistance genes. *The ISME Journal* 9, 2490.
- Liao, H., Lu, X., Rensing, C., Friman, V.P., Geisen, S., Chen, Z., et al., 2018. Hyperthermophilic composting accelerates the removal of antibiotic resistance genes and mobile genetic elements in sewage sludge. *Environmental Science & Technology* 52 (1), 266–276.
- Liu, Y., Zhang, Y., Ni, B.J., 2015. Zero valent iron simultaneously enhances methane production and sulfate reduction in anaerobic granular sludge reactors. *Water Res.* 75, 292.
- Ma, Y., Wilson, C.A., Novak, J.T., Riffat, R., Aynur, S., Murthy, S., et al., 2011. Effect of various sludge digestion conditions on sulfonamide, macrolide, and tetracycline resistance genes and class 1 integrons. *Environmental Science & Technology* 45, 7855–7861.
- Ma, J., Gu, J., Wang, X., Peng, H., Wang, Q., Zhang, R., et al., 2019. Effects of nano-zerovalent iron on antibiotic resistance genes during the anaerobic digestion of cattle manure. *Bioresour. Technol.* 289.
- Mager, D.M., Thomas, A.D., 2011. Extracellular polysaccharides from cyanobacterial soil crusts: a review of their role in dryland soil processes. *J. Arid Environ.* 75, 91–97.
- Miller, J.H., Novak, J.T., Knocke, W.R., Pruden, A., 2015. Elevation of antibiotic resistance genes at cold temperatures: implications for winter storage of sludge and biosolids. *Lett. Appl. Microbiol.* 59, 587–593.
- Munck, C., Albertsen, M., Telke, A., Ellabaan, M., Nielsen, P.H., Sommer, M.O.A., 2015. Limited dissemination of the wastewater treatment plant core resistome. *Nat. Commun.* 6, 8452.
- Organization, W.H., 2015. WHO | Global Action Plan on Antimicrobial Resistance.
- Pan, X., Lv, N., Li, C., Ning, J., Wang, T., Wang, R., et al., 2019. Impact of nano zero valent iron on tetracycline degradation and microbial community succession during anaerobic digestion. *Chem. Eng. J.* 359, 662–671.
- Qiao, M., Ying, G.-G., Singer, A.C., Zhu, Y.-G., 2017. Review of antibiotic resistance in China and its environment. *Environ. Int.* 110, 160–172.
- Rasheed, R., Khan, N., Yasar, A., Su, Y.H., Tabinda, A.B.J.R.E., 2016. Design and cost-benefit analysis of a novel anaerobic industrial bioenergy plant in Pakistan. *Renew. Energy* 90, 242–247.
- Rudnick, H., Hendrich, S., Pilatus, U., Blotvogel, K.H., 1990. Phosphate accumulation and the occurrence of polyphosphates and cyclic 2,3-diphosphoglycerate in *Methanosarcina frisia*. *Arch. Microbiol.* 154, 584–588.
- Shi, J.H., Su, Y.L., Zhang, Z.J., Wei, H.W., Xie, B., 2019. How do zinc oxide and zero valent iron nanoparticles impact the occurrence of antibiotic resistance genes in landfill leachate? *Environmental Science-Nano* 6, 2141–2151.
- Song, W., Wang, X., Gu, J., Zhang, S., Yin, Y., Li, Y., et al., 2017. Effects of different swine manure to wheat straw ratios on antibiotic resistance genes and the microbial community structure during anaerobic digestion. *Bioresour. Technol.* 231, 1–8.
- Srilakshmi, K., Sierra-Alvarez, R., Field, J.A., 2010. Zero valent iron as an electron-donor for methanogenesis and sulfate reduction in anaerobic sludge. *Biotechnol. Bioeng.* 92, 810–819.
- Suanon, F., Sun, Q., Mama, D., Li, J., Dimon, B., Yu, C.P., 2016. Effect of nanoscale zero-valent iron and magnetite (Fe₃O₄) on the fate of metals during anaerobic digestion of sludge. *Water Res.* 88, 897.
- Sui, Q., Zhang, J., Chen, M., Tong, J., Wang, R., Wei, Y., 2016. Distribution of antibiotic resistance genes (ARGs) in anaerobic digestion and land application of swine wastewater. *Environ. Pollut.* 213, 751–759.
- Su-Li, M.A., Liu, H., Yan, Q., 2011. Effect of Fe-(2+) concentration on the enzymes during methane production from Taihu blue algae by anaerobic digestion. *Journal of Food Science & Biotechnology* 30, 306–310.
- Tong, J., Lu, X., Zhang, J., Angelidaki, I., Wei, Y., 2018. Factors influencing the fate of antibiotic resistance genes during thermochemical pretreatment and anaerobic digestion of pharmaceutical waste sludge. *Environ. Pollut.* 243.
- Wang, T., Zhang, D., Dai, L., Dong, B., Dai, X., 2018. Magnetite triggering enhanced DIET: a scavenger for the blockage of electron transfer in anaerobic digestion of high-solids sewage sludge. *Environmental Science & Technology* 52.
- Wright, G.D., 2010. Antibiotic resistance in the environment: a link to the clinic? *Curr. Opin. Microbiol.* 13, 589.
- Wu, D., Huang, X.H., Sun, J.Z., Graham, D.W., Xie, B., 2017. Antibiotic resistance genes and associated microbial community conditions in aging landfill systems. *Environmental Science & Technology* 51, 12859–12867.
- Xiang, Y., Yang, Z., Zhang, Y., Xu, R., Zheng, Y., Hu, J., et al., 2019. Influence of nanoscale zero-valent iron and magnetite nanoparticles on anaerobic digestion performance and macrolide, aminoglycoside, beta-lactam resistance genes reduction. *Bioresour. Technol.* 294, 122139.
- Xu, R., Yang, Z.-H., Wang, Q.-P., Bai, Y., Liu, J.-B., Zheng, Y., et al., 2018a. Rapid startup of thermophilic anaerobic digester to remove tetracycline and sulfonamides resistance genes from sewage sludge. *Sci. Total Environ.* 612, 788–798.
- Xu, R., Yang, Z.H., Zheng, Y., Liu, J.B., Xiong, W.P., Zhang, Y.R., et al., 2018b. Organic loading rate and hydraulic retention time shape distinct ecological networks of anaerobic digestion related microbiome. *Bioresour. Technol.* 262, 184.
- Xu, R., Xu, S., Zhang, L., Florentino, A.P., Yang, Z., Liu, Y., 2019. Impact of zero valent iron on Blackwater anaerobic digestion. *Bioresour. Technol.* 285, 121351.
- Yang, Z.-H., Xu, R., Zheng, Y., Chen, T., Zhao, L.-J., Li, M., 2016a. Characterization of extracellular polymeric substances and microbial diversity in anaerobic co-digestion reactor treated sewage sludge with fat, oil, grease. *Bioresour. Technol.* 212, 164–173.
- Yang, Z., Guo, R., Shi, X., Wang, C., Wang, L., Dai, M., 2016b. Magnetite nanoparticles enable a rapid conversion of volatile fatty acids to methane. *RSC Adv.* 6, 25662–25668.
- Zhang, J., Le, Z., Loh, K.C., Dai, Y., Tong, Y.W., 2017. Enhanced anaerobic digestion of food waste by adding activated carbon: fate of bacterial pathogens and antibiotic resistance genes. *Biochem. Eng. J.* 128 (S1369703X17302243).
- Zhang, J., Wang, Z., Lu, T., Liu, J., Wang, Y., Shen, P., et al., 2019a. Response and mechanisms of the performance and fate of antibiotic resistance genes to nano-magnetite during anaerobic digestion of swine manure. *J. Hazard. Mater.* 366, 192–201.
- Zhang, Y., Yang, Z., Xu, R., Xiang, Y., Jia, M., Hu, J., et al., 2019b. Enhanced mesophilic anaerobic digestion of waste sludge with the iron nanoparticles addition and kinetic analysis. *Sci. Total Environ.* 683, 124–133.
- Zhao, Y., Cocerva, T., Cox, S., Tardif, S., Su, J.Q., Zhu, Y.G., et al., 2019. Evidence for co-selection of antibiotic resistance genes and mobile genetic elements in metal polluted urban soils. *Sci. Total Environ.* 656, 512–520.
- Zhu, L., Gao, K., Jin, J., Lin, H., Xu, X., 2014. Analysis of ZVI corrosion products and their functions in the combined ZVI and anaerobic sludge system. *Environ. Sci. Pollut. Res.* 21, 12747–12756.